



HAL
open science

Phase transitions and dielectric relaxations in superionic protonic conductor HUP ($\text{H}_3\text{O}^+\text{UO}_2\text{PO}_4 \cdot 3\text{H}_2\text{O}$) in the broad frequency range (10⁻²-10¹⁰ Hz)

J.C. Badot, A. Fourier-Lamer, N. Baffier, Ph. Colomban

► To cite this version:

J.C. Badot, A. Fourier-Lamer, N. Baffier, Ph. Colomban. Phase transitions and dielectric relaxations in superionic protonic conductor HUP ($\text{H}_3\text{O}^+\text{UO}_2\text{PO}_4 \cdot 3\text{H}_2\text{O}$) in the broad frequency range (10⁻²-10¹⁰ Hz). *Journal de Physique*, 1987, 48 (8), pp.1325-1336. 10.1051/jphys:019870048080132500 . jpa-00210559

HAL Id: jpa-00210559

<https://hal.science/jpa-00210559>

Submitted on 4 Feb 2008

HAL is a multi-disciplinary open access archive for the deposit and dissemination of scientific research documents, whether they are published or not. The documents may come from teaching and research institutions in France or abroad, or from public or private research centers.

L'archive ouverte pluridisciplinaire **HAL**, est destinée au dépôt et à la diffusion de documents scientifiques de niveau recherche, publiés ou non, émanant des établissements d'enseignement et de recherche français ou étrangers, des laboratoires publics ou privés.

Classification
Physics Abstracts
77.40

Phase transitions and dielectric relaxations in superionic protonic conductor HUP ($\text{H}_3\text{OUO}_2\text{PO}_4 \cdot 3\text{H}_2\text{O}$) in the broad frequency range (10^{-2} - 10^{10} Hz)

J. C. Badot ^(a), A. Fourier-Lamer ^(b), N. Baffier ^(a) and Ph. Colomban ^(c)

^(a) Laboratoire de Chimie de la Matière Condensée, UA 302/CNRS ENSCP, 11, rue P.-et-M.-Curie, 75231 Paris Cedex 05, France

^(b) Laboratoire de Dispositifs Infrarouges, UA 836/CNRS Université P. et M. Curie, T. 12 E. 2, 4, place Jussieu, 75005 Paris, France

^(c) Groupe de Chimie du Solide, Laboratoire de Physique de la Matière Condensée, GR 038/CNRS, Ecole Polytechnique, 91128 Palaiseau, France

(Reçu le 27 janvier 1987, accepté le 6 avril 1987)

Résumé. — Les propriétés diélectriques du phosphate d'uranyle hydraté d'oxonium (HUP = $\text{H}_3\text{OUO}_2\text{PO}_4 \cdot 3\text{H}_2\text{O}$) et de son dérivé (NaUP = $\text{NaUO}_2\text{PO}_4 \cdot 3\text{H}_2\text{O}$) sous forme d'échantillons denses, polycristallins, préparés par frittage sous charge à 25 °C ont été étudiées entre 10^{-2} et 10^{10} Hz. Trois ou deux relaxations dipolaires différentes ont été observées pour HUP ou NaUP respectivement et attribuées aux processus de réorientation des espèces protoniques (H_2O , H_3O^+), aux sauts des ions H_3O^+ ou aux molécules d'eau couplées aux ions conducteurs. Les relations entre relaxation dipolaire, ferroélectricité et superconduction ionique sont discutées.

Abstract. — The dielectric properties of hydrogen uranyle phosphate (HUP = $\text{H}_3\text{OUO}_2\text{PO}_4 \cdot 3\text{H}_2\text{O}$) and its sodium homologous (NaUP = $\text{NaUO}_2\text{PO}_4 \cdot 3\text{H}_2\text{O}$) have been studied between 10^{-2} and 10^{10} Hz. The samples are dense polycrystalline pellets sintered under pressure at 25 °C. Three or two dipolar relaxations are observed for HUP or NaUP respectively and assigned to protonic species reorientations (H_2O , H_3O^+), to H_3O^+ ions or to ions coupled water molecules jumps. Dipolar relaxation, ferroelectricity and superionic conductivity are discussed.

1. Introduction.

$\text{H}_3\text{OUO}_2\text{PO}_4 \cdot 3\text{H}_2\text{O}$ (Hydrogen Uranyl Phosphate = HUP) is the best known proton solid conductor ($\sigma_{RT} \sim 6 \times 10^{-3} \Omega^{-1} \text{cm}^{-1}$) and is used in microionic devices such as electrochromic displays, sensors, batteries or supercapacitors [1-4]. The structure consists of infinite sheets of $(\text{UO}_2\text{PO}_4)_n$ entities separated by a two-level water molecules layer (Fig. 1), oxygen atoms of this layer form squares and are hydrogen-bonded [5-6], one of the four water molecules being replaced by an H_3O^+ ion. H_3O^+ ions can be exchanged by Na^+ , K^+ , NH_4^+ ... ions and these materials also exhibit ionic conductivity [7]. Furthermore, HUP undergoes several phase transitions: a paraelectric/ferroelectric transition about 260 K [8] and two weaker transitions at about 220 K and 110 K [9], respectively. These transitions corre-

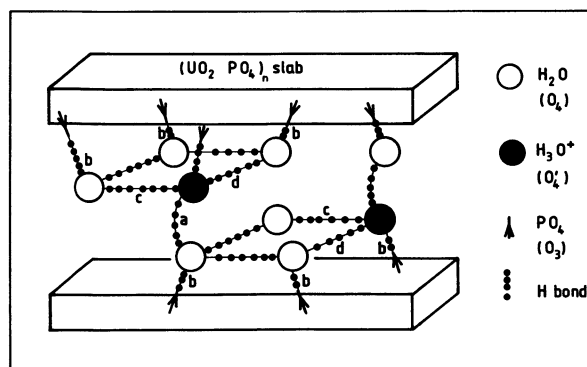


Fig. 1. — Schematic structure of water layer in $\text{H}_3\text{OUO}_2\text{PO}_4$.

spond to the freezing of the various degrees of freedom for the protonic species around the hydro-

gen bonds. The structure varies from an ordered (hydrogen bonded) water molecule layer below 110 K to a quasi liquid state between the $(\text{UO}_2\text{PO}_4)_n$ slabs at room temperature.

A dielectric study in the broad frequency range has recently been performed on $\text{V}_2\text{O}_5\text{-}1.6\text{H}_2\text{O}$ xerogels [10] in order to discern the dielectric relaxation of the various protonic species present in the gels and has demonstrated the potentiality of the method for the study of protonic conductors. HUP is presently considered as a model for the understanding of the « wet » superprotonic conduction in well crystallized materials. In this paper, we search to determine the dielectric relaxation of each protonic species in comparison with previous spectroscopic studies. The comparison between NaUP and HUP allows to discriminate between ions and water motions, and to contribute to a better description of the conductivity mechanism.

2. Experimental.

2.1 MATERIALS SYNTHESIS. — Microcrystalline powder of HUP is synthesized from equimolar (2.3 M) aqueous solutions of H_3PO_4 and uranyl nitrate at room temperature. The washing of the powder must be carefully controlled in order to avoid a degradation of the surface materials which can be transformed in $(\text{UO}_2)_{1.5-x}\text{PO}_4\text{H}_{2x}\cdot 3\text{H}_2\text{O}$ [11]. These gradual modifications of the material lower the conductivity (as shown in Fig. 2) and smooth the para/ferroelectric transition. NaUP isomorph (and KUP) is obtained by ionic exchange in convenient NaNO_3 (and KNO_3) aqueous solution [7].

2.2 ELECTRICAL MEASUREMENTS.

2.2.1 Low frequency range (10^{-2} - 10^6 Hz). — Conductivity is determined by mean of the complex impedance method: a Solartron (Schlumberg Inc) impedance analyser monitored by an Apple II microcomputer is used. In preliminar experiments, electrodes are Pt foils deposited at the surface of steel plugs which are also used to pressure-sintered the HUP materials in the form of disks (200 kg/cm^2). Translucent pellets ($\varnothing 10\text{ mm}$, thickness 3-4 mm) are obtained. Preferable orientation occurs with the c axis — perpendicular to the $(\text{UO}_2\text{PO}_4)_n$ sheets — parallel to the pressing direction. This effect would slightly lower the conductivity value down to the single crystal conductivity value [7, 12]. However, we have obtained $Z'' = f(Z')$ spectra (Fig. 3a and 3b) which have shown a nearly continuous feature which makes difficult the interpretation of the diagram. Thus we have used in high frequency range (see further 2.2.2) thin film ($\sim 0.1\text{ mm}$) of a composite electrode made of a mixing of HUP and

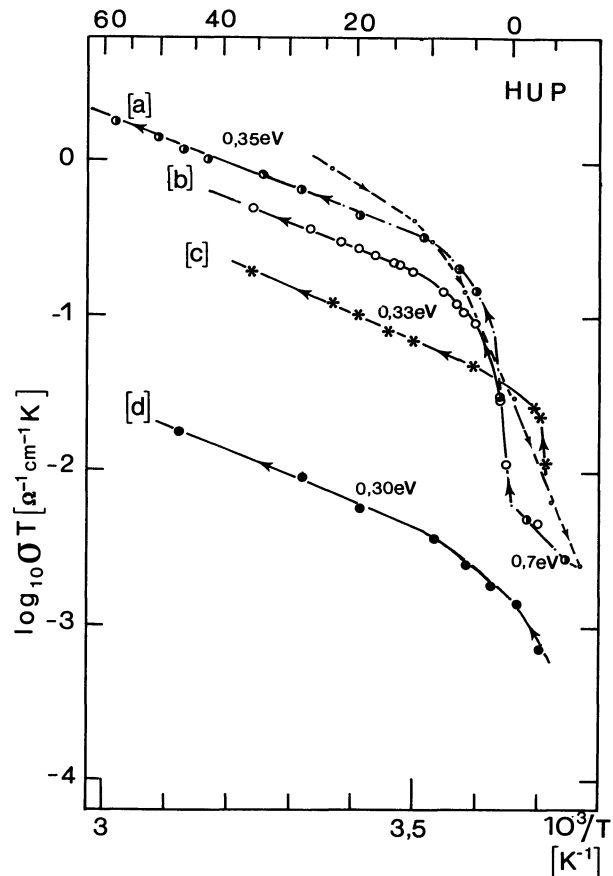


Fig. 2. — Influence of the washing on HUP dc conductivity: (a) optical clear pressure sintered pellet; (b) pellet made with powder washed with H_2O during 2 h; (c) pellet made with powder washed with H_2O during 10 h; stacking faults are formed; (d) opaque pellet prepared and washed with H_2O during a few days; the crystallinity is lowered and the structure is partly destroyed [11].

carbone in defined proportion, corresponding to the double percolation of the electrolyte (HUP) and of the electronic conductor (black carbon) (Fig. 4) [13]. The films are deposited on both surfaces of the precompact pellet and after that the final composition is made. Complex impedance analysis were performed between 260 K and 340 K under N_2 flux.

2.2.2 High frequency range. — The study of the real and imaginary parts of the complex dielectric permittivity $\varepsilon^*(\omega)$ was performed in the 100 kHz to 12 GHz range with the following apparatus:

- between 100 kHz and 1 MHz = LF impedance analyzer model HP 4192 A
- between 1 MHz and 1 GHz = RF impedance analyzer model HP 4191 A
- between 1 GHz and 12 GHz = network analyzers model HP 8746.

HUP and NaUP samples are compacted pellets with a diameter $2a = 3\text{ mm}$ and a thickness $d = 1\text{ mm}$. The preliminar experiments, made with

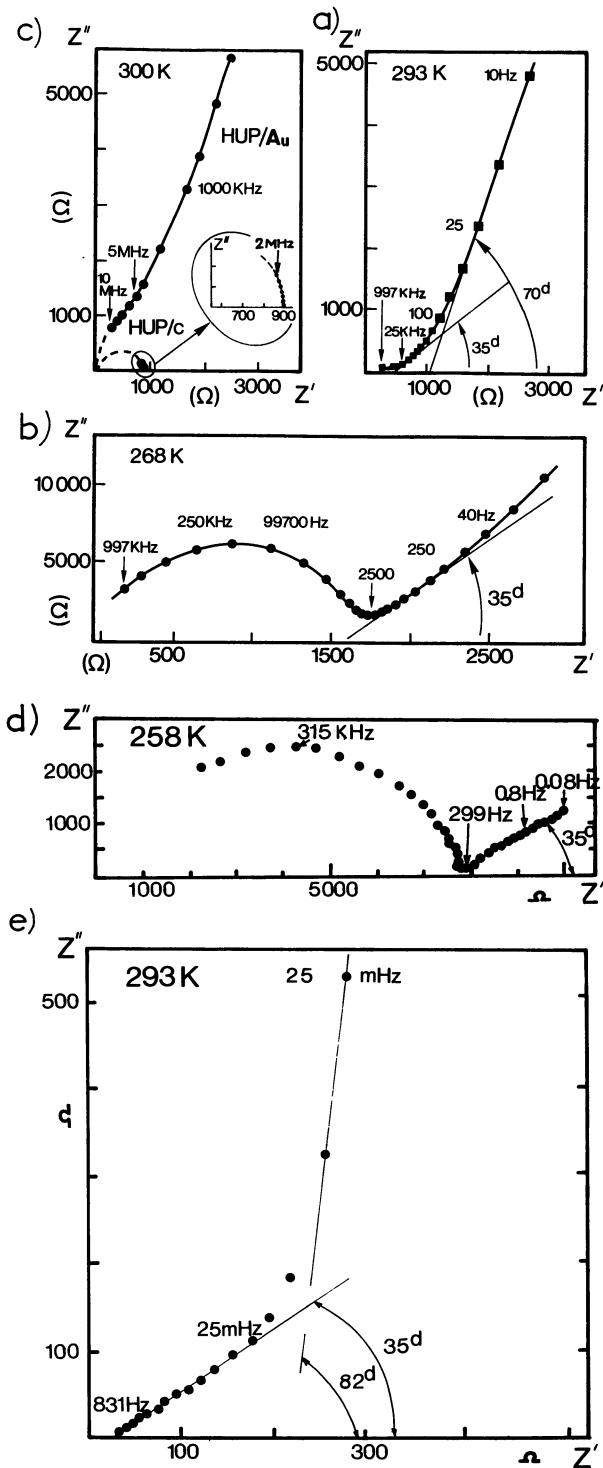


Fig. 3. — Complex impedance diagrams ($Z'' = f(Z')$) for HUP: influence of the electrodes on the electrical measurements: (a) Pt foils at 293 K; (b) Pt foils at 268 K; (c) Brass/Au plugs (up) and Norit RBX/HUP composite electrodes (down) at $T = 300$ K; (d) Norit RBX/HUP composite electrodes at $T = 258$ K; (e) Norit RBX/HUP composite electrodes at $T = 293$ K.

Brass plugs covered with Au thin film electrodes, have shown that the interfacial phenomena were preponderant up to 10 MHz (Fig. 3c). This effect

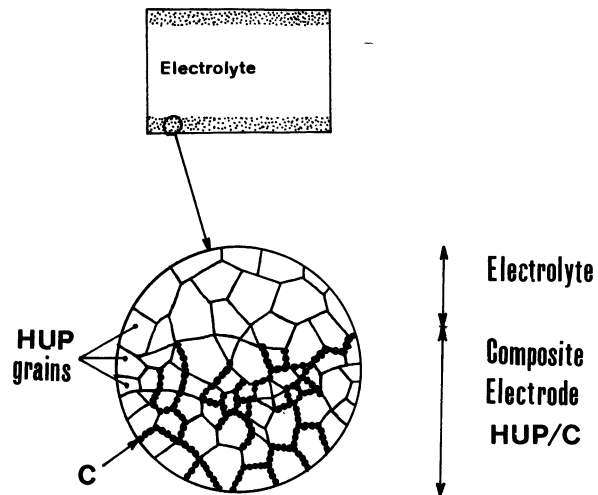


Fig. 4. — Schematic representation of the microstructure of the HUP/C composite electrode.

masks the bulk properties which could appear in the 1 MHz-10 MHz range (semi-circle in complex impedance representation $Z'' = f(Z')$). Thus we have used, as for low frequency range measurements, a thin film of a composite electrode made of a mixing of HUP and carbone (NORIT RBX) deposited on both surfaces of the precompact pellet. The results are more reliable, as observed in figure 3c.

The cell is a circular coaxial line whose inner conductor is interrupted by the sample (Fig. 5a and 5b). It is loaded with the characteristic impedance Z_0 ($Z_0 = 50 \Omega$).

3. Results and discussion.

3.1 SEPARATION BETWEEN BULK AND INTERFACIAL PHENOMENA. —

The study of the electrical properties of ionic conductors — or electronic insulators — involves difficulties in realization of electrodes. In the case of the electronic conductors, the contact with a metallic electrode is easily ohmic. However in the case of ionic conductors, it is more difficult to obtain a good contact even if the physical contact is realized between electrode and electrolyte. As protonic conductors are easily decomposed with temperature or small partial water-pressure, it is impossible to use gold coatings under vacuum. Utilization of silver lacquered electrodes is also prohibited owing to the possible chemical reactions (solvent reactions, ionic exchange). However one can use Pt foils or composite electrodes made of a mixture of electrolyte and carbon leading to the percolation of carbon grains [13].

Furthermore the electrical measurement must not perturb the electrolyte: small values of the voltages (~ 10 mV) are required, lower than those involving an electro-reduction (> 1 V for H_2O and hydrates).

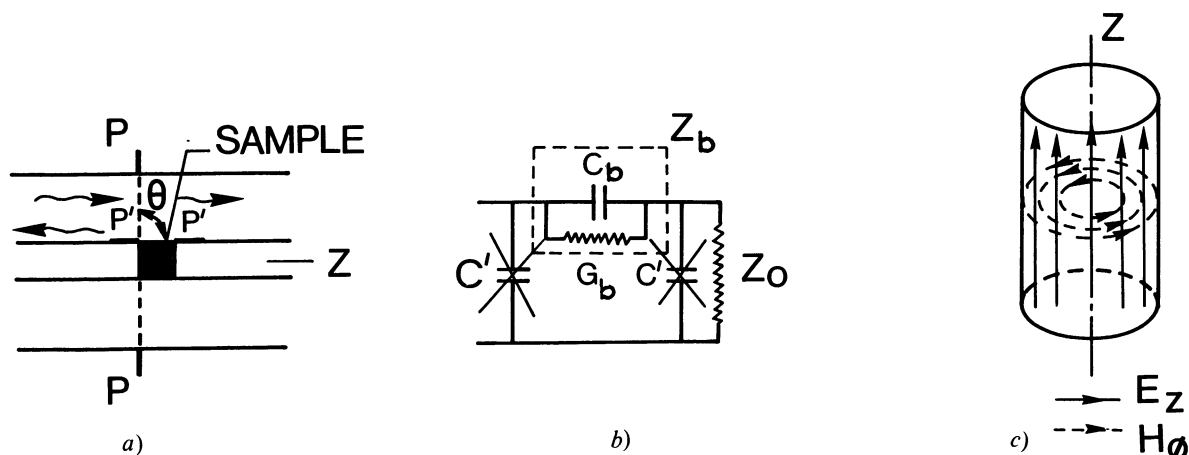


Fig. 5. — High frequency measurement cell : (a) sample loaded with the characteristic impedance Z_0 ; (b) equivalent network corresponding to (a) ; (c) sample electromagnetic field distribution.

It is difficult to know the real contact area which can play a part in interfacial phenomena. But as the electrode resistance is negligible towards electrolyte resistance, the total conductivity of the sample does not vary more than one half order of magnitude whatever the nature of the electrode may be, whereas the presence of chemical defects can involve variation within one order of magnitude (Fig. 2). Furthermore it is important to avoid imperfections such as the porosity due to an incomplete compactness of the pellets.

It is important to observe all the different relaxations which can exist in a sample in order to have a

full approach of these phenomena. Therefore the relaxations due to interfaces — according to the nature of the electrodes occur in different frequency domains making then difficult the observation of all phenomena.

3.1.1 Low frequency range ($10^{-2} < f < 10^6$ Hz).

3.1.1.1 Measurement window with usual Pt electrode. — Figures 6 and 7 compare Bode conductivity plots for HUP, NaUP and KUP at various temperatures — real part $G(\omega)$ and imaginary part $B(\omega)$ of the admittance $Y^*(\omega) = G(\omega) + iB(\omega)$ vs. frequency $f = \omega / 2\pi$. Figure 8a shows the equivalent

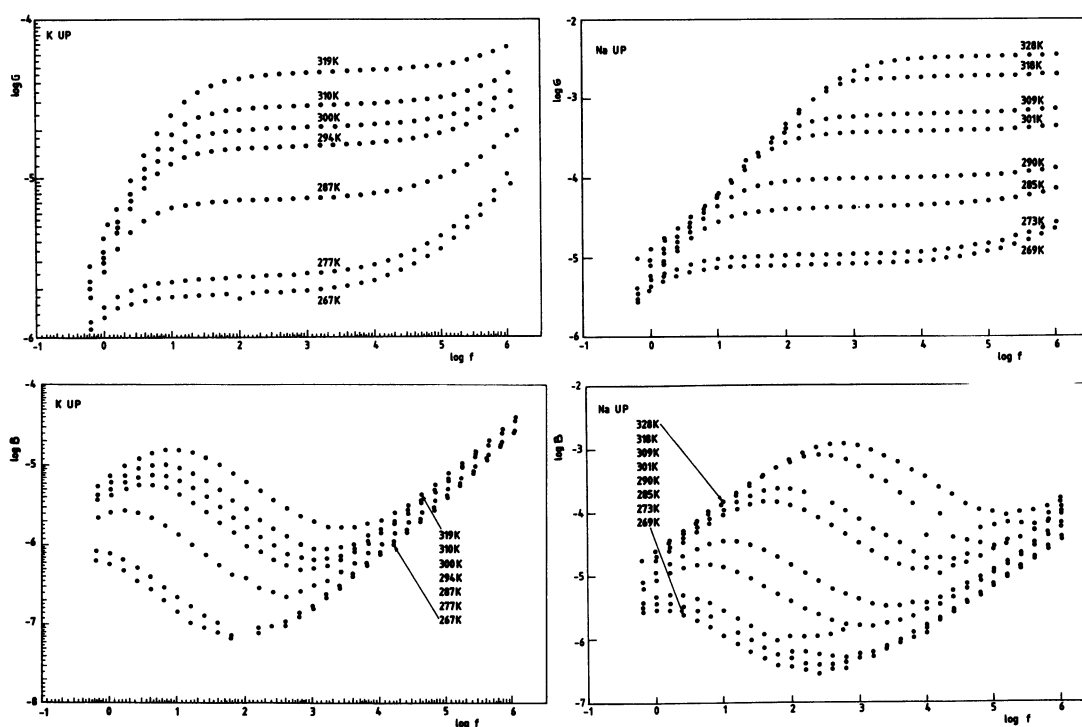


Fig. 6. — Bode-conductivity^a log plots (real part $G(\omega)$ and imaginary part $B(\omega)$ of the admittance $Y^*(\omega)$ vs. frequency $f = \omega / 2\pi$ for NaUP and KUP at various temperatures (G is given in $\Omega^{-1} \cdot \text{cm}^{-1}$).

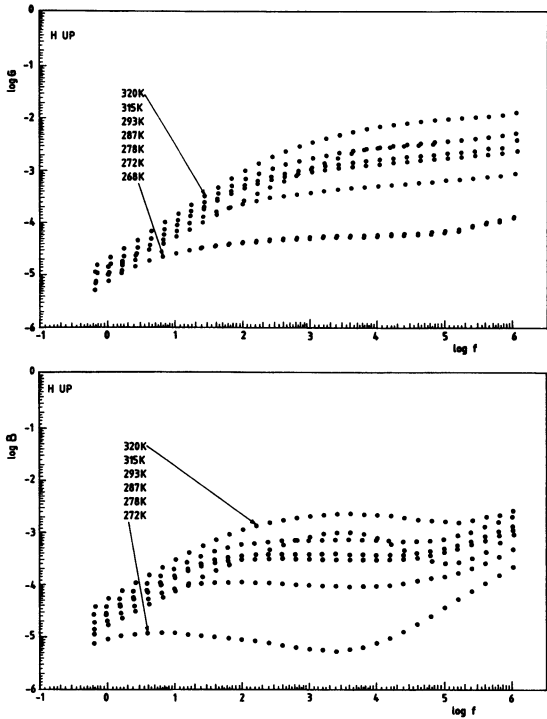


Fig. 7. — Bode-conductivity log plots (real part $G(\omega)$ and imaginary part $B(\omega)$ of the admittance $Y^*(\omega)$ vs. frequency $f = \omega / 2 \pi$ for HUP at various temperatures (G is given in $\Omega^{-1} \cdot \text{cm}^{-1}$)

network of the system where the bulk resistance R_b is related to the conductivity of the solid electrolyte $R_b = d/\sigma S$ ($S =$ sample surface, $d =$ sample thickness, $\sigma \sim$ d.c. conductivity $\sigma(0)$), C_i is the interfacial capacity (typically a few $\mu\text{F}/\text{cm}^2$), C_g is the geometric capacity (a few pF) related to the dielectric permittivity of the solid electrolyte — $C_g = \epsilon_0 \epsilon S/d$ —, R_e is the electrode resistance. R_e is negligible at low frequencies and C_g plays a role only at high frequencies, i.e. when $C_g \omega \approx 1/R_b$.

At lower frequencies :

$$Y^*(\omega) = G(\omega) + iB(\omega) = \frac{R_b C_i^2 \omega^2}{1 + R_b^2 C_i^2 \omega^2} + i \frac{C_i \omega}{1 + R_b^2 C_i^2 \omega^2} \quad (1)$$

If we compare HUP, NaUP and KUP plots (Figs. 6 and 7), an horizontal line is well observed, due to the bulk conductivity of the materials (4×10^{-3} , 10^{-4} and $5 \times 10^{-6} \Omega^{-1} \text{cm}^{-1}$ at 290 K for HUP, NaUP and KUP respectively, the temperature dependence of HUP is given in figure 2, according to previous works [7]. Moreover, the figure clearly shows the phase transition occurring for HUP below 270 K. However, the slope of $G(\omega)$ in the low frequency range is nearly 1 ($G(\omega) \approx A\omega$) and not 2 as expected from the equation ($G(\omega) \approx R_b C_i^2 \omega^2$)

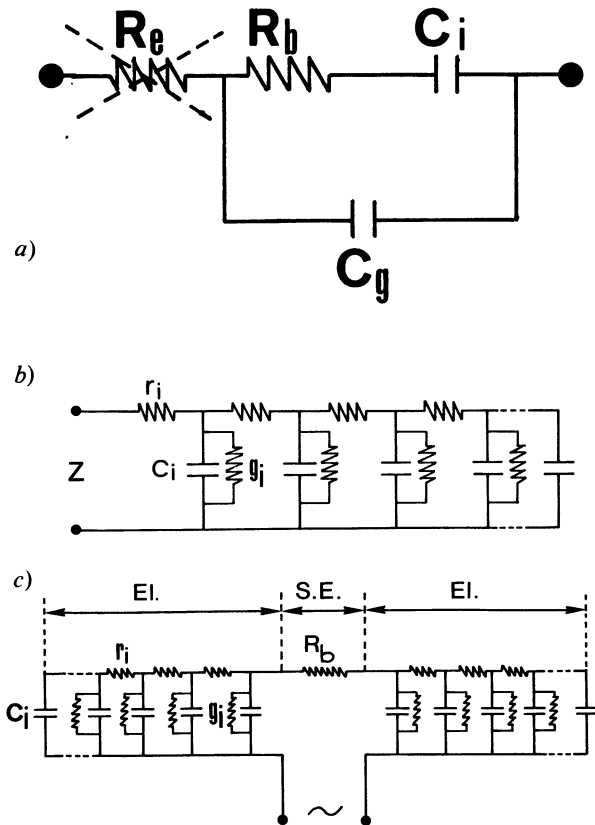


Fig. 8. — Equivalent networks in the low frequency range ($10^{-2} \text{ Hz} - 10^6 \text{ Hz}$) : (a) HUP sample with Pt foil electrode ; (b) Norit RBX/HUP composite electrode ; (c) HUP sample with composite electrodes ; (d) Theoretical diagram of the infinite transmission line.

when $\omega \rightarrow 0$). This phenomenon has already been observed in other superionic conductors [14] and assigned to interfacial charge transfer due to an additional capacity in parallel with C_i . Some authors [15] replace C_i by an interfacial impedance $Z_i^*(\omega) = A(i\omega)^{-p}$ where p is an empirical parameter. They always obtain a p value lower than 1 and close to 0.8-0.9. The meaning of this value is not well established although some authors attempt to explain it by the universal law of Jonscher [16] or by fractal models [17].

If we compare the imaginary part $B(\omega)$ of KUP and NaUP the observed plots are consistent with the above description. At lower frequencies, the slope is 1 ($B(\omega) \approx C_i \omega$); then, after the maximum occurring at $\omega = 1/R_b C_i$, a -1 slope is observed ($B(\omega) \approx 1/R_b C_i \omega$). This maximum is lowered with temperature. In the high frequency range ($\omega > 10^5$ Hz), the geometric capacity ($B(\omega) \approx C_g \omega$) becomes predominant for the poor conductors.

In the case of HUP, the situation is more complex and the 1, -1 slopes are not well characterized.

For the study of the bulk behaviour, it is thus necessary to shift these extrinsic phenomena (i.e. the low frequency interfacial phenomena) to very low frequencies using composite electrodes.

3.1.1.2 Composite HUP/C electrodes. — The low frequency interfacial phenomenon can be shifted to very low frequency domain when composite electrodes are used. The figure 3 compares $Z'' = f(Z')$ plots of HUP solid electrolyte performed using Pt foils (Fig. 3a and 3b) or HUP/C composite electrodes (Fig. 3d and 3e).

The impedance diagram $Z'' = f(Z')$ recorded with Norit RBX/HUP composites electrodes [4, 13, 18] shows two straight lines parts with 35° and 82° angle respectively. Figure 8b and figure 8c show the theoretical equivalent network of the composite electrode and of the two composite electrodes with the pure electrolyte membrane respectively: the frequency dependence of the interaction sample/electrodes is represented by two identical infinite transmission lines with characteristic impedance Z_0 in series with the resistance R_b which represents the sample in the very low frequency domain. To account for the local microstructure and the double percolation carbon/HUP, we have defined characteristic impedance Z_0 with the expression $Z_0 = [r_i/(g_i + ic_i \omega)]^{1/2}$ where r_i and g_i could be associated with different conductivities of carbon and HUP respectively, c_i is the lineic capacity associated with the effective permittivity of the composite. When the frequency is varying, the diagram $Z'' = f(Z')$ is given in figure 8d. This diagram shows two straight lines one is vertical (low frequency range of the diagram) and the other has a

slope of 45° . This theoretical diagram allows the calculus of R_b , r_i , c_i , g_i . The experimental results show a departure from this model: two straight lines with 35° (high frequency range) and 82° (low frequency range) angles respectively (Fig. 3). These various slopes can be related to the ratio of characteristic length of the local microstructure and the mean displacement of the alternating charge: this behaviour is similar to that usually observed in the case of porous or composite electrodes [19-21]. Insertion phenomena on non ideally blocking electrode are also a possible explanation. Using a phenomenological description, the impedance law is thus $Z \approx A(i\omega)^{-p}$ (the 35° and 82° values lead to $p \approx 0.4$ and $p \approx 0.9$ respectively). The relaxation times of the charge transfer phenomena are shifted from ≈ 300 kHz to 300 Hz when the capacity increases from a factor 3×10^3 , due to the large surface of the HUP/C interface.

3.1.2 High frequency range ($f > 10^6$ Hz). — In this frequency domain, the study of the bulk dielectric relaxation is possible only when using composite electrodes. In the sample, the electric field is parallel to the common axis of the sample and the inner conductor (Fig. 5a and 5c), as fully described in [10]. The impedance Z_b of the sample is connected in series with the load in the P' plane tangential to the cylindrical sample. The impedance defined in this plane is $Z_{p'} = Z_0 + Z_b$. From Z_p measured in the phase reference plane P, $Z_{p'}$ is determined when Z_b is lower than the impedance between inner and outer conductors as precedently discussed in [10, 22]. The knowledge of Z_b allows the determination of the dielectric permittivity ϵ' and the dielectric loss or imaginary part ϵ'' as detailed in [10, 23]. The complex permittivity is:

$$\epsilon^*(\omega) = \epsilon'(\omega) - i\epsilon''(\omega).$$

For frequencies below 1 GHz, Z_b is proportional to the complex resistivity ρ^* as described in [10] by

$$Z_b = \frac{1}{i\omega} \cdot \frac{1}{\epsilon_0 \epsilon^*} \cdot \frac{d}{\pi a^2} = \rho^*(\omega) \frac{d}{\pi a^2}. \quad (2)$$

In this frequency domain, it is thus possible to use complex impedance representation ($Z'' = f(Z')$) for determining the direct current resistivity $\rho(0)$. However, above 1 GHz, this representation is not correct while Z and ρ^* are not proportional as previously described in [10, 23].

The conventional model used in the description of the dielectric relaxation is the Debye model [24] which gives the frequency dependent complex permittivity with an equation of the form:

$$\frac{\epsilon^*(\omega) - \epsilon_\infty}{\epsilon_s - \epsilon_\infty} = \frac{1}{1 + i\omega\tau} \quad (3)$$

where ϵ_∞ and ϵ_s are limit values of $\epsilon^*(\omega)$ as ω approaches $+\infty$ and 0 respectively. τ is known as the Debye relaxation time and $f_p = 1/(2\pi\tau)$ is the loss peak frequency. The relaxation time τ is a measure of the nominal time scale on which molecular reorientation can take place. If the dipoles interact with each other, the used equation is slightly different :

$$\frac{\epsilon^*(\omega) - \epsilon_\infty}{\epsilon_s - \epsilon_\infty} = \frac{1}{1 + (i\omega\tau)^{1-\alpha}} \quad (4)$$

where α is an empirical parameter ($0 < \alpha < 1$) which measures the degree of departure from Debye model [10, 16, 24, 25].

The relaxation time can be deduced from the frequency $f = 1/(2\pi\tau)$ corresponding to the point of the semi-circle with abscissa $(\epsilon_s + \epsilon_\infty)/2$.

The relative experimental errors in ϵ' and ϵ'' are approximately 2% for lower frequencies and 5% for higher frequencies.

3.2 EVIDENCE OF VARIOUS RELAXATIONS AND PHASE TRANSITIONS. — Figure 9 compares typical Cole-Cole plots ($\epsilon'' = f(\epsilon')$) for HUP and NaUP at

various temperatures between 190 K and 300 K. The decomposition of these plots reveals two distinct kinds of behaviour : one is represented by a straight line (domain 1), as observed in low frequency analysis and the other by semi-circles or circular arcs (domains 2, 3 and 4 in HUP, 2 and 3 in NaUP) characterizing dielectric relaxations.

At 300 K the ϵ'' values are very high for HUP and NaUP, in the low frequency range (Fig. 9a). Thus, for convenience, ϵ'' values corresponding to domain 1 have been subtracted from the experimental values (Fig. 9d and 9f). In our case the decomposition is almost straight forward but, in our previous work [10], where the relaxations are not so clearly defined, the decomposition procedure has been extensively discussed. Our experimental results — for HUP and NaUP — are given in table I.

— *Domain 1* : in the case of HUP and NaUP this domain occurs in the low frequency range and is represented by a (quasi) vertical straight line.

— *Domain 2* : this domain occurs in the middle frequency range and is represented by semi-circle arcs characterizing quasi-Debye dielectric relaxation ($\alpha \approx 0$). We notice that the relaxation time τ_2 (see

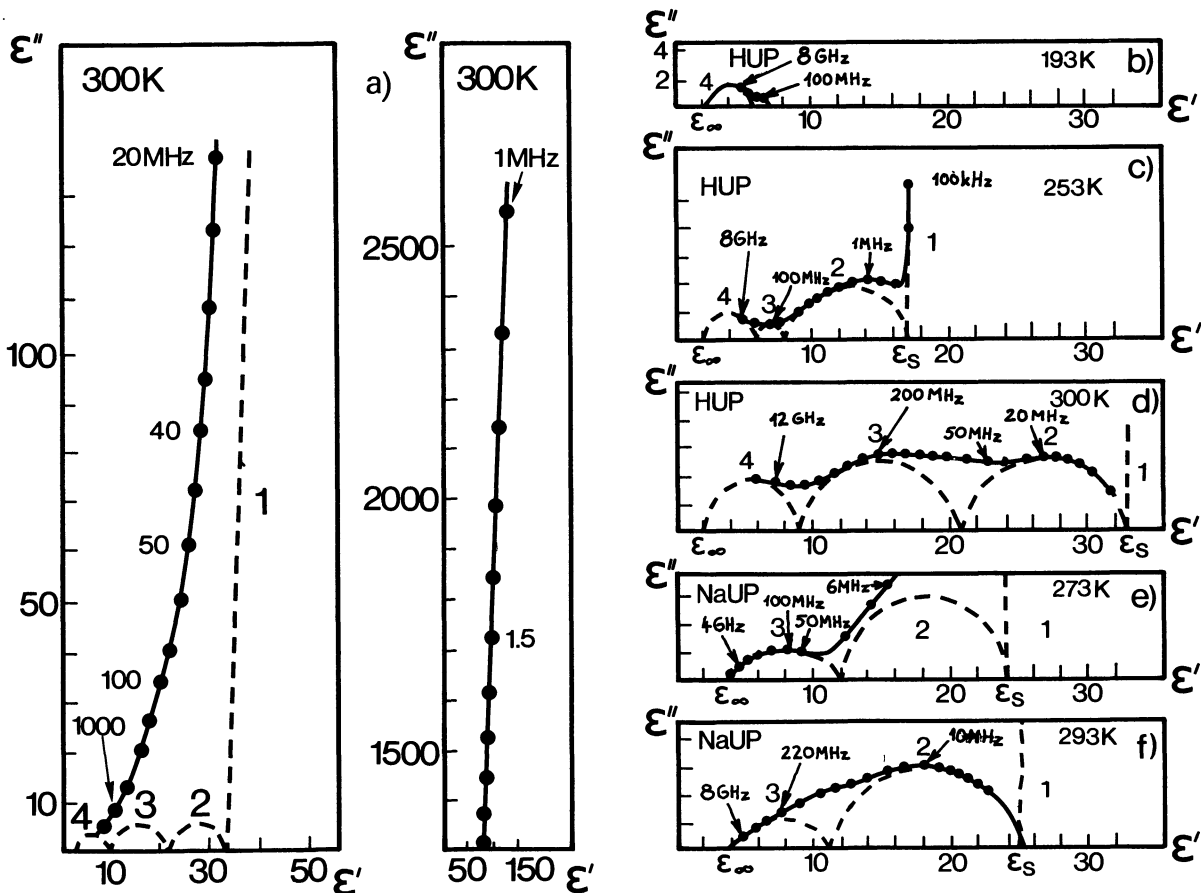


Fig. 9. — Cole-Cole plots $\epsilon'' = f(\epsilon')$: (a) HUP, $T = 300$ K (whole frequency range); (b) HUP, $T = 193$ K; (c) HUP, $T = 253$ K; (d) HUP, $T = 300$ K (contribution of domain 1 is subtracted for convenience); (e) NaUP, $T = 273$ K; (f) NaUP, $T = 293$ K (contribution of domain 1 is subtracted for convenience); experimental errors on ϵ' and ϵ'' (2.5%) are not specified for clarity.

Tab. I) is strongly lowered with increasing temperature. Figure 10 compares the evolutions of τ_2 as a function of the inverse temperature in the case of NaUP and HUP. The temperature dependence of τ_2 follows an Arrhenius law (except in the transition range 270-265 K of HUP): $\tau_2 = \tau_0 \exp(E/kT)$. Currently E is considered as the activation energy for the molecule reorientation (or charge hopping) and the prefactor τ_0 is the inverse of the oscillation frequency of the dipole (or charge) in its potential well.

— *Domains 3 and 4*: these domains occur in the high frequency range and are represented by circular

arcs characterizing Debye-type relaxations [24] (Fig. 9). The domain 4 is not observed in NaUP, which indicates that this phenomenon is likely related to H_3O^+ species. The temperature dependence of the relaxation time τ_3 follows an Arrhenius law with an activation energy 0.25 eV (Tab. I and Fig. 10). In other words, temperature dependence of τ_3 and τ_4 in HUP exhibits a more complex behaviour: i) an Arrhenius behaviour in phase I ($T > 270$ K) with activation energies $E_3 = 0.23$ eV and $E_4 = 0.13$ eV respectively; ii) a non-Arrhenius behaviour in phases II ($215 < T < 270$ K) and III ($T < 215$ K).

Table I. — *Different parameters obtained in HUP and NaUP.*

HUP	T/K	τ/s	τ'/s	E/eV	$\Delta\epsilon$	ϵ_s	ϵ_∞
Domain 4 H_3O^+ reorientation	300	7.96×10^{-12}	5×10^{-12}	0.13	6.6		2
	290	9.37×10^{-12}	6.36×10^{-12}		7		
	278	1.22×10^{-11}	8×10^{-12}		8		
	268	1.6×10^{-11}	9.16×10^{-12}		6		
	263	1.24×10^{-11}	10^{-11}		7		
	253	10^{-11}	1.28×10^{-11}		4		
	243	1.15×10^{-11}			4		
	213	1.6×10^{-11}			3		
	193	1.27×10^{-11}			3		
Domain 3 H_2O reorientation	300	7.2×10^{-10}	2.4×10^{-10}	0.25	12		
	290	8.8×10^{-10}	3.2×10^{-10}		13		
	278	1.6×10^{-9}	5×10^{-9}		17		
	268	2.2×10^{-9}	1.3×10^{-9}		6		
	263	1.6×10^{-9}	1.6×10^{-9}		4		
	253	8×10^{-10}	2.5×10^{-9}		2.2		
	243	8×10^{-10}			1.8		
	213	10^{-9}			1		
	193	10^{-9}			1		
Domain 2 $\text{H}_3\text{O}^+/\text{H}_2\text{O}$ jump	300	8×10^{-9}		0.34	12	31	
	290	1.26×10^{-8}			14	34	
	278	3.2×10^{-8}			16	41	
	268	4.3×10^{-8}			54	66	
	263	5×10^{-8}			26	35	
	253	10^{-7}			9	22	
	243	2.5×10^{-7}			9	15	

NaUP	T/K	τ/s	E/eV	$\Delta\epsilon$	ϵ_s	ϵ_∞
Domain 3 H_2O reorientation	293	7.2×10^{-10}	0.25	8		4
	284	1.1×10^{-9}		8		
	273	1.6×10^{-9}		7.5		
Domain 2 $\text{Na}^+/\text{H}_2\text{O}$ jump	293	1.6×10^{-8}	0.45	12	24	
	284	3.5×10^{-8}		11.5	23.5	
	273	8×10^{-8}		13	24.5	

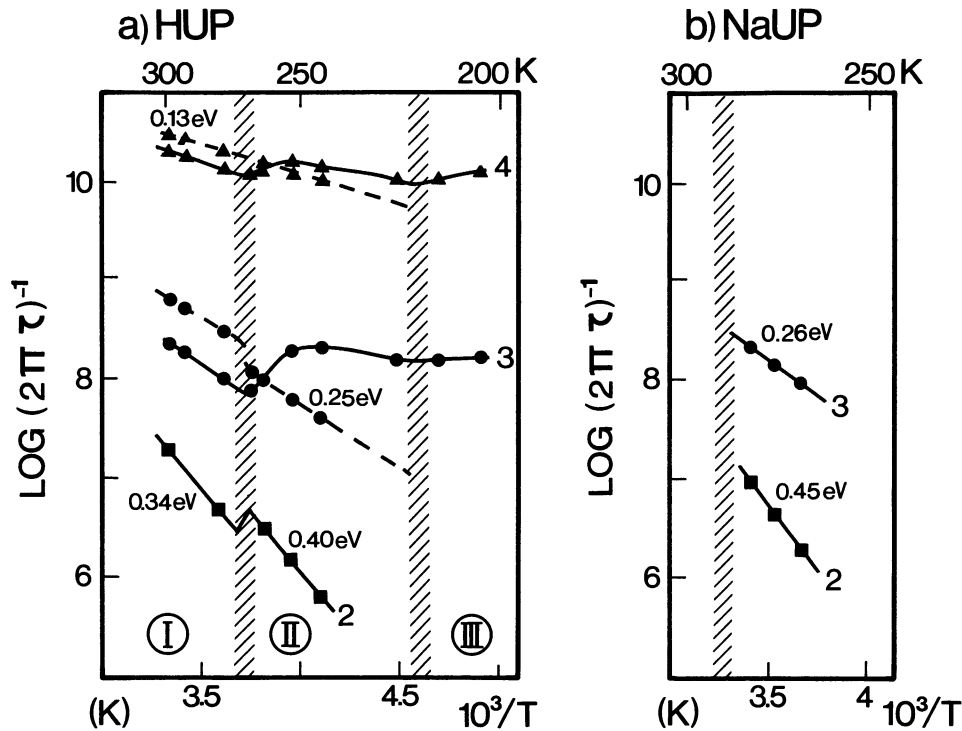


Fig. 10. — Temperature dependence of relaxation frequency $f_p = (2\pi\tau)^{-1}$: (a) HUP, domain 2 (■), domain 3 (●), domain 4 (▲); (b) NaUP, domain 2 (■), domain 3 (●) with $(2\pi\tau)^{-1}$ (—) and $(2\pi\tau)^{-1}$ (- - -).

The figure 11 compares the ϵ_s variations of NaUP and HUP with inverse temperature and the reciprocal dielectric susceptibility $(\Delta\epsilon)^{-1} = (\epsilon_s - \epsilon_\infty)^{-1}$ with temperature.

We observe that :

- i) $1/\Delta\epsilon$ is constant in the whole temperature range for NaUP.
- ii) $1/\Delta\epsilon$ exhibits a minimum at the para/ferroelectric transition of HUP samples.

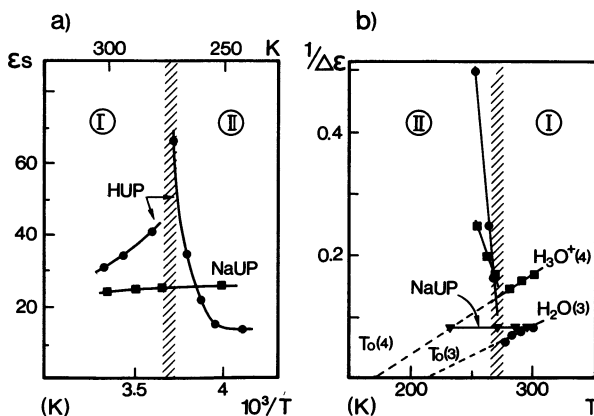


Fig. 11. — (a) Inverse temperature dependence of static permittivity ϵ_s of HUP (●) and NaUP (■); (b) temperature dependence of reciprocal dielectric permittivity $1/\Delta\epsilon$ for domain 3 in HUP (●), domain 4 in HUP (■), domain 3 in NaUP (▼). T_0 are the extrapolated Curie Weiss temperatures.

3.3 ASSIGNMENT OF RELAXATIONS.

3.3.1 « Direct » current conductivity. — The Cole-Cole plot of domain 1 represented by a (quasi) vertical straight line corresponds to the « direct » current conductivity $\sigma(\omega \rightarrow 0)$ or $\sigma(0)$. This behaviour corresponds to the circular arc observed in complex impedance representation ($Z'' = f(Z')$) shown in figure 3c. The choice of blocking carbon electrodes allows to determine the direct-current resistance $R(0)$ at the intersection of circular arc with Z' axis.

The temperature dependence of the conductivity is $\sigma T = A \exp(-E_1/kT)$ where E_1 is the activation energy of the conductivity. According to previous studies [7, 9, 12, 26], the activation energy for HUP material is 0.34 eV above 270 K and 0.75 eV below 260 K. At 300 K, the ionic conductivity of small pellets is about $3 \times 10^{-3} \Omega^{-1} \text{cm}^{-1}$ in agreement with the value measured on larger perfectly densified pellets ($6 \times 10^{-3} \Omega^{-1} \text{cm}^{-1}$). In the case of NaUP material, the average activation energy is about ≈ 0.78 eV in agreement with the previous determination [7]; at 300 K the value of the conductivity is about $2 \times 10^{-4} \Omega^{-1} \text{cm}^{-1}$.

3.3.2 Space-charge relaxation. — (Quasi-) Debye relaxation could be due to space-charge relaxation or to local motions [27]. With no applied electric field, charges are uniformly distributed in the sample. When an electric field is applied, charges are localized in the sample under the action of the

field and the diffusion gradient. By reversal of the field, the charges undergo a new equilibrium so that the new macroscopic dipole — whose dimension is the same as the sample thickness — and the new polarisation are opposed to the previous ones. Thus, a Debye-type dielectric relaxation is established, due to the switching of the macroscopic dipole whose frequency varies with the inverse of the sample thickness. Table II compares the results for domain 2 in NaUP and HUP samples of different thickness, 0.5 and 1 mm respectively. This clearly shows that results are not affected by the thickness. In conclusion no space charge relaxation is observed for low-frequency part (domain 2) in our spectra. Thus the observed (quasi-) Debye relaxation corresponding to domain 2 is due to local motions.

Table II. — *Relaxation frequency of domain 2 (HUP, NaUP) for samples of thickness 0,5 and 1 mm.*

d/mm	F_p/MHz HUP	F_p/MHz NaUP
1	20	10
0,5	20	10

3.3.3 Local motions and ions jumps. — The dielectric relaxation associated with hopping ionic conduction has been extensively discussed [28-32]. The ionic conductivity is shown to have the following frequency dependence :

$$\begin{aligned} \sigma(\omega) &= \sigma(0) + \omega \varepsilon''(\omega) = \\ &= \sigma(\infty) - \frac{\sigma(\infty) - \sigma(0)}{1 + \omega^2 \tau^2} \quad (5) \end{aligned}$$

where $\sigma(0)$ is the d.c. conductivity observed in the domain 1 ($\sigma = \sigma(0)$ when $\omega\tau \ll 1$), $\varepsilon''(\omega)$ is the dielectric loss and $\sigma(\infty)$ is the high frequency conductivity when $\omega\tau \gg 1$.

Interactions between the ions — nearest neighbour interactions —, structure with inequivalent sites and hopping involving the motion of large number of ionic species introduce correlations between subsequent jumps. These effects must yield a conductivity which increases with frequency and satisfies the equation (5). One can argue that if an ion hops from site i to site j , one expects the ion to be « bounced-back » to site i whenever interactions are present. This « bounced back » effect [29] tends to reduce that the d.c. conductivity $\sigma(0)$ relative to high frequency conductivity $\sigma(\infty)$. Thus, there is some coupling effect between long range motion (low frequencies) and local hopping (high frequencies). The relaxation time τ (cf. Eq. (5)) is the time corresponding to the « bounced back » effect.

Activation energies of the d.c. conductivity

$\sigma(0)$ and of the relaxation (domain 2) are the same (0.3 eV) in the high temperature phase I of HUP, which supports the assignment of domain 2 to H_3O^+ jump. The relaxation time τ_2 is nearly equal to 10^{-8} s at 300 K. This value is in good agreement with quasielastic neutron scattering experiments performed on HUP [33] and on other superionic conductors such as e.g. NH_4^+ β alumina [34]. For $T < 270$ K (phase II), comparison between the activation energy of the d.c. conductivity $\sigma(0)$ (0.75 eV) and that of the relaxation (0.4 eV) shows some discrepancy.

In NaUP the activation energy of relaxation has a value nearly equal to 0.45 eV (Na^+ jumps) which corresponds to the $\sigma(0)$ value determined in the high temperature phase ($T > 310$ K) [6]. For $T < 310$ K the same comparison as for HUP can be made between the activation energies of the conductivity $\sigma(0)$ (0.78 eV) and of the relaxation (0.43 eV).

In both cases (HUP at $T < 270$ K and NaUP at $T < 310$ K), the low temperature activation energy of $\sigma(0)$ is nearly equal to the sum of the ions (H_3O^+ and Na^+) and of H_2O jump activation energies.

3.3.4 Protonic species reorientations. — In HUP, with the existence of both H_3O^+ and H_2O species, we may consider three types of motions :

- i) hopping of H_2O or H_3O^+ species as discussed above ;
- ii) reorientation of the dipolar H_3O^+ ion ;
- iii) reorientation of the water molecules.

We notice that the domains 2 and 3 of HUP and NaUP are similar as far as activation energies and relaxation times are concerned. It seems thus reasonable to assign the relaxations 3 and 4 to H_2O reorientation, whereas domain 4 corresponds more likely to H_3O^+ reorientation. The activation energy for dielectric relaxation of the water molecule is related to the local crystalline field and to the possibility to establish hydrogen bond.

Activation energy (E_3) for these relaxations are nearly equal to 0.25 eV in NaUP and HUP (phase I). This is consistent with previous spectroscopic studies [6, 9] which showed that the local environment is almost unchanged, the variation being dynamical. However the increased value of the relaxation time ($\tau_3 \approx 8 \times 10^{-10}$ s at 300 K) for the water molecules in NaUP and HUP, with respect to the relaxation time of the liquid water, is two orders of magnitude. This value is in good agreement with previous quasi elastic neutron scattering (QNS) experiment for both HUP [33] and NaUP [35]. This can be related to the coupling of quasi-liquid protonated water layer with $(\text{UO}_2\text{PO}_4)_n$ sheet which « freezes » the proton dynamic. The relaxation time

measured on HUP ($\tau_4 \sim 8 \times 10^{-12}$ s at 300 K) and assigned to H_3O^+ reorientation is also in good agreement with the value deduced for the same motion from QNS measurements [33].

3.4 FERROELECTRIC RELAXATION IN HUP. — The ferroelectric behaviour of $\text{H}_3\text{OUO}_2\text{AsO}_4 \cdot 3\text{H}_2\text{O}$ isomorph is well established [8]. On the other hand, the ferroelectric properties of HUP have been deduced from structural isomorphism and from the frequency dependence conductivity below 260 K in the case of a single frequency four-point measurement [12]. From Z'' and Z' measurements on HUP samples under a small static electric field (1 V/mm), we have observed a shift of the I-II transition to about 290 K, which demonstrates that the I-II transition is of paraelectric — ferroelectric type [36, 37]. Figure 11 shows the evolution of the reciprocal dielectric susceptibility $1/\Delta\epsilon$ in the case of the domains 3 and 4. A Curie Weiss law $1/\Delta\epsilon = 1/C^{-1}(T - T_0)$ is well observed in the paraelectric phase I for both domains. The extrapolated Curie Weiss temperatures T_0 are about 210 K and 170 K for H_2O (domain 3) and H_3O^+ (domain 4) dipoles respectively, the C constant being approximatively 10^3 K for the two dipoles. Thus, this I-II transition is a first order transition because T_0 are lower than the transition temperature 270 K, according to calorimetric study [6].

The relaxation times τ_3 and τ_4 assigned respectively to H_2O and H_3O^+ reorientations are characterized by a « critical slowing-down » (cf. Fig. 10) which has been previously observed in ferroelectric relaxation of H-bonded ferroelectrics [38, 39]. These relaxation times are defined by collective mechanisms of molecular reorientation involving long-range interaction of dipole-dipole type. From Ising model and molecular field approximation [39], one can define a relaxation time τ' (i.e. τ'_3, τ'_4) characterizing the individual reorientation of each molecule when no interaction between dipoles is established :

$$\tau' = \frac{C}{T} \cdot \frac{1}{\Delta\epsilon} \cdot \tau \quad (6)$$

where C is the Curie constant, $\Delta\epsilon$ the dielectric susceptibility and τ the measured relaxation time.

The τ' values (τ'_3, τ'_4) have been reported on table I and figure 10 for the domains 3 and 4. These

τ' values which account for individual molecular motions are in better agreement with QNS experiments [33] than τ values : 2.4×10^{-10} s and 5×10^{-12} s for H_2O and H_3O^+ respectively compared with 10^{-10} s and 4×10^{-12} s obtained by QNS experiments. The temperature dependences of τ'_3 and τ'_4 are in this way of Arrhenius-type in both phases I and II. It is then possible to determine the activation energies of reorientation for H_2O and H_3O^+ dipoles : 0.25 eV and 0.13 eV in the two phases respectively. We conclude that the local environment remains unchanged through the phase transition, which confirms the previous spectroscopic study in the same temperature range [6, 9].

4. Conclusion.

The study of dielectric relaxation of protonic conductors appears as an exciting method for the comprehension of proton dynamics. This method is easier to apply than quasi-elastic neutron scattering (QNS) and provides similar results. In the case of uranyl hydrate superionic conductor we are able to observe the successive phase transitions and to separate :

- i) low-frequency effect due to the diffusion of charge carriers (H_3O^+ or Na^+ ions) ;
- ii) dielectric relaxations due to H_3O^+ jumps (or H_3O^+ - H_2O coupled jumps) and Na^+ - H_2O coupled jumps ;
- iii) dielectric relaxations due to H_3O^+ or H_2O reorientations.

The activation energies observed for ions jumps are in good agreement with long distance (low-frequency) charge transfer, which is consistent with our interpretation of protonic conductivity in HUP with an usual ion jump model. The smaller reorientation time for H_2O in HUP than in NaUP is related to the conductivity difference. The Grotthus model is possible only for HUP as a complementary and secondary mechanism. This mechanism is enhanced with the small reorientation time of H_3O^+ ions.

Acknowledgments.

We have enjoyed very useful discussions with Dr. M. Pham-Thi.

References

- [1] HOWE, A. T., SHEFFIELD, S. H., CHILDS, P. E. and SHILTON, M. G., *Thin Solid Films* **67** (1980) 365.
- [2] VELASCO, G., PERTHUIS, H. and COLOMBAN, Ph. in *Proc. Int. Meet. on Chemical Sensors*, Fukuoka, Sept. 19-27 1983, Seiyama T., Fuekik., Shiohawa J. and Suzuki S. Eds. (Elsevier Amsterdam) 1983, p. 239.
- [3] KAHIL, H., FORESTIER, M. and GUITTON, J. in *Solid State Protonic Conductors III*, Goodenough, J. B., Potier, A. and Jensen, J., Eds. (Odense University Press) 1985, p. 356.
- [4] PHAM-THI, M., ADET, Ph., VELASCO, G. and COLOMBAN, Ph., *Appl. Phys. Lett.* **48** (1986) 1348.
- [5] MOROSIN, B., *Phys. Lett. A* **65** (1978) 53.

- [6] PHAM-THI, M., COLOMBAN, Ph. and NOVAK, A., *J. Phys. Chem. Solids* **46** (1985) 493 and *ibid* 565.
- [7] PHAM-THI, M. and COLOMBAN, Ph., *Solid State Ionics* **17** (1985) 295.
- [8] DE BENYACAR, M. A. R. and DE DUSSEL, H. L., *Ferroelectrics* **9** (1975) 241.
- [9] COLOMBAN, Ph., PHAM-THI, M. and NOVAK, A., *Solid State Commun.* **53** (1985) 747.
- [10] BADOT, J. C., FOURRIER-LAMER, A. and BAFFIER, N., *J. Physique* **46** (1985) 2107.
- [11] PHAM-THI, M. and COLOMBAN, Ph., *J. Less. Common Met.* **108** (1985) 189.
- [12] HOWE, A. T. and SHILTON, M. G., *J. Solid State Chem.* **34** (1980) 149.
- [13] PHAM-THI, M., VELASCO, G. and COLOMBAN, Ph., *J. Mater. Sci. Lett.* **5** (1986) 415.
- [14] SALARDENNE, J. and COUTURIER, G., *De la microélectronique à la microionique*, Ph. Colomban Ed. (1983) p. 189-197.
- [15] FUNKE, K., *Solid State Ionics* **18-19** (1986) 183-190.
- [16] JONSHER, A. K., *J. Mater. Sci.* **16** (1981) 2037.
- [17] LIU, S. H., KAPLAN, T. and GRAY, L. J., *Solid State Ionics* **18-19** (1986) 65-71.
- [18] PHAM-THI, M., Thesis, University of Montpellier (1985).
- [19] HO, C., RAISTRICK, I. D. and HUGGINS, R. A., *J. Electrochem. Soc.* **127** (1980) 343-350.
- [20] THOMAS, M. G. S. R., BRUCE, P. G. and GOODENOUGH, J. B., *J. Electrochem. Soc.* **132** (1985) 1521-1528.
- [21] SUCHANSKI, M. R., *J. Electrochem. Soc.* **132** (1985) 2059-2063.
- [22] GETSINGER, W. J., *IEEE Trans. Microwave Theory Tech.* **MTT-14** (1966) 58.
- [23] KOLODZIEJ, H., SOBSCYK, L., *Acta Phys. Pol.* **A 39** (1971) 59.
- [24] DEBYE, P., *Polar Molecules* (Dower, New York) 1945.
- [25] COLE, K. S. and COLE, R. H., *J. Chem. Phys.* **2** (1941) 341.
- [26] KREUER, K. D., RABENAU, A. and MESSER, R., *Appl. Phys.* **A 32** (1983) 45 and *ibid.* 155.
- [27] COELHO, R., *Revue Phys. Appl.* **18** (1983) 137-146.
- [28] HUBER, D. L., *Phys. Rev.* **B 15** (1977) 533.
- [29] RICHARDS, P. M., *Phys. Rev.* **B 16** (1977) 1393.
- [30] KIMBALL, J. C. and ADAMS, L. W., Jr, *Phys. Rev.* **B 18** (1978) 5851.
- [31] PIETRONERO, L., STRAESSLER, S. and ZELLER, H. R., *Fast ion transport in solids*, Eds. P. Vashista, J. N. Mundy and G. K. Shenoy (North Holland) 1979, p. 165.
- [32] WONG, T. and BRODWIN, M., *Solid State Commun.* **36** (1980) 503-508.
- [33] POINSIGNON, C., FITCH, A. and FEUDER, B. E. F., *Solid State Ionics* **9-10** (1983) 1049.
- [34] LASSEGUES, J. C., FOUASSIER, M., BAFFIER, N., COLOMBAN, Ph. and DIANOUX, A. J., *J. Physique* **41** (1980) 273.
- [35] POINSIGNON, C., FITCH, A. and COLOMBAN, Ph., *J. Physique* (submitted).
- [36] BENGUIGUI, L., Thesis (1969) Paris.
- [37] FATUZZO, E. and MERZ, W. J., *Ferroelectricity* (North Holland Publishing Company, Amsterdam) 1967, p. 121.
- [38] KOLODZIEJ, H., *Dielectric and related molecular processes*, vol. 2, Ed. Davies, M. (London Chemical Society) 1975, p. 249.
- [39] MAKITA, Y. and SEO, I., *J. Chem. Phys.* **51** (1969) 3058.
-